Quantitative study of effects of free cationic chains on gene transfection in different intracellular stages

Jinge Cai [a,*], Yanan Yue [a], Yanjing Wang [a], Zhenyu Jin [b], Fan Jin [b], Chi Wu [a,c,**]

[a] Department of Chemistry, The Chinese University of Hong Kong, Shatin, N.T., Hong Kong
[b] Hefei National Laboratory for Physical Sciences at the Microscale, University of Science and Technology of China, Hefei, Anhui 230026, China
[c] Hefei National Laboratory of Physical Science at the Microscale, Department of Chemical Physics, University of Science and Technology of China, Hefei, Anhui 230026, China

ABSTRACT

Previously, we revealed that in the application of using cationic polymer chains, polyethylenimine (PEI), to condense anionic plasmid DNA chains (pDNA) to form the DNA/polymer polyplexes, after all the pDNAs are complexed with PEI, further added PEIs exist individual chains and free in the solution mixture. It is those uncomplexed polycation chains that dramatically promote the gene transfection. In the current study, we studied how those free cationic chains with different lengths and topologies affect the intracellular trafficking of the polyplexes, the translocation of pDNA through the nuclear membrane, the transcription of pDNA to mRNA and the translocation of mRNA from nucleus to cytosol in HepG2 cells by using a combination of the three-dimensional confocal microscope and TaqMan real-time PCR. We found that free branched PEI chains with a molar mass of 25,000 g/mol and a total concentration of 1.8×10^{-6} g/mL promote the overall gene transfection efficiency by a factor of ~500 times. Our results quantitatively reveal that free chains help little in the cellular uptake, but clearly reduce the lysosomal entrapment of those internalized polyplexes (2–3 folds); assist the translocation of pDNA through nuclear membrane after it is released from the polyplexes in the cytosol (~5 folds); enhance the pDNA-to-mRNA transcription efficiency (~4 folds); and facilitate the nucleus-to-cytosol translocation of mRNA (7–8 folds). The total enhancement of those steps agrees well with the overall efficiency, demonstrating, *for the first time,* how free cationic polymer chains quantitatively promote the gene transfection in each step in the intracellular space.

© 2016 Elsevier B.V. All rights reserved.

1. Introduction

Even after extensive studies over the last several decades, clinically delivering therapeutic genes still remains a challenge [1–4]. In comparison with small cationic surfactant molecules, different cationic polymers as potentially useful non-viral vectors have also attracted much attentions, presumably due to their low immune toxicity, structure flexibility and commercial viability [5–8]. In a typical cationic polymer gene delivery system, cationic chains neutralize anionic charges on plasmid DNA (pDNA) chains, resulting in the contraction of both polymer and DNA chains to form large DNA/polymer complexes (often called as polyplexes) with a size around $\sim 10^2$ nm. The process is driven by the translational entropy gain of those released small counter ions, rather than the electrostatic attraction often described in literature [9,10]. The complexation reduces the degradation of DNA and facilitates the

gene delivery. However, one big piece missed in such a complicated gene transfection puzzle is how large polyplexes travel in the intracellular space, including their cytosol transportation and nuclear entry.

Our recent studies revealed that in a typical transfection-effective mixture of polymers and DNA chains (the molar ratio of nitrogen from polycation to phosphate from pDNA, N/P ~ 10), only ~30% of cationic chains are required to fully condense long anionic pDNA chains and each polyplex on average contains only one pDNA chain [11,12]. In other words, ~70% of added cationic chains are free in the solution mixture of polymer and pDNA. Further, we clearly demonstrated that the cationic chains free in the solution mixture and bound to pDNAs play two distinct roles in an effective transfection process [11,12]. Namely, the bound chains only play a charge-neutrality role in condensing and stabilizing each complexed DNA chain during the cellular uptake and intracellular trafficking; and it is those free cationic chains that promote the gene transfection by $\sim 10^2$ folds [11–13]. Hitherto, nearly all of previous studies in developing polymer vectors have not realized such two functional roles of the cationic chains. Therefore, it is important to elucidate the detailed mechanism of how free cationic polymer chains promote the gene transfection in order to design an efficient cationic polymer vector.

* Corresponding author.
** Correspondence to: C. Wu, Department of Chemistry, The Chinese University of Hong Kong, Shatin, N.T., Hong Kong.
E-mail addresses: caijinge@gmail.com (J. Cai), chiwu@cuhk.edu.hk (C. Wu).

Among various kinds of cationic polymers, polyethylenimine (PEI) still stands out as a "golden standard" nowadays for the gene delivery study in spite of its cytotoxicity in real biomedical applications because of their high transfection efficiency and well-documented synthesis [14–16]. It has been previously proven that PEI chains are fully complexed with pDNAs to form the polyplexes when the N/P ratio reaches ~3 but the solution mixture with N/P ~ 10 is ~10^2 times more effective in the gene transfection [12,13]. Putting these two experimental results together, one should logically and naturally conclude that the additional 7 portion of cationic chains must remain free in the solution mixture of polymer and pDNA; and it is them that promote the gene transfection. In addition, the length and topology of free cationic chains also remarkably affect the overall gene transfection efficiency [17–19]. However, a quantitative elucidation of how cationic free chains promote the gene transfection at each intracellular stage, such as the avoidance of the lysosomal entrapment, the translocation of pDNA through the nuclear membrane, the transcription and the translocation of mRNA from nucleus to cytosol remains a challenge.

In the current study, we used branched PEIs with a weight-average molar mass M_w of ~25,000 g/mol (b25k-PEIs) to condense pDNAs to form the polyplexes with a size of ~10^2 nm and several PEIs with different lengths and topologies as free chains to promote the gene transfection. The choice of b25k-PEI as the bound chains is due to its higher binding affinity so that they will not be replaced by those further added free cationic chains in the solution mixtures [13]. In this way, we can focus on the quantitative effects of those free cationic chains on each step of gene transfection, which includes the cellular uptake and the lysosomal entrapment/degradation of the polyplexes, the translocation of pDNA through nuclear membrane and the transcription of pDNA, the translocation of mRNA and the final translation [20–24], by using a combination of confocal microscopy and TaqMan real-time PCR. The cumulated effect of free chains in promoting gene transfection in each individual step is compared with the overall gene transfection efficiency, leading, *for the first time*, to a better understanding of how polymer vectors work inside the intracellular space.

2. Materials and methods

2.1. Materials and cell lines

Branched polyethylenimine (PEI) with a weight-average molar mass (M_w) of 2000 g/mol (b2k-PEI, Sigma-Aldrich) was freeze-dried prior to use. Branched PEI ($M_w = 25,000$ g/mol, b25k-PEI, Sigma-Aldrich) and two linear PEI samples ($M_w = 2500$ and 25,000 g/mol, lin2.5k-PEI and lin25k-PEI, Polysciences) were used without further purification. The initial plasmid DNA (pDNA) pGL3-control vector (5256 bp) encoding a modified coding region for firefly luciferase and pEGFP-N1 (4700 bp) expressing enhanced green fluorescent protein were purchased from Promega (USA) and Clontech (Germany), respectively. Large amounts of pDNAs were prepared with Qiagen plasmid maxi kit (Qiagen, Germany) according to the manufacturer's instructions. 5-(N, N-Hexamethylene) amiloride (HMA), wortmannin (Wort), and chlorpromazine hydrochloride (Chlp) were purchased from Sigma-Aldrich (Germany). Fetal bovine serum (FBS), Dulbecco's modified Eagle's medium (DMEM) and penicillin-streptomycin were purchased from Gibco (USA). HepG2 cells were grown at 37 °C, 5% CO_2 in DMEM medium supplemented with 10% FBS, penicillin at 100 units/mL and streptomycin at 100 μg/mL.

2.2. Formation of pDNA/b25k-PEI polyplexes

The pDNAs were complexed with b25k-PEIs to form the pDNA/b25k-PEI polyplexes at N/P = 3. An equal volume of a b25k-PEI solution (1.6 μg/mL) in phosphate buffered saline (PBS) was added dropwise into a pDNA PBS solution (4.0 μg/mL). The resultant 10× polyplexes solution mixture was incubated at room temperature for 5 min before further dilution for the gene transfection.

2.3. In vitro gene transfection

The in vitro transgene expression was quantified by the luciferase assay system (Promega, USA) in HepG2 cells with pGL3 as the exogenous reporter gene. 24 h before the gene transfection, HepG2 cells were seeded in a 48-well plate at a density of 12,000 cells per well in 200 μL of the DMEM complete medium. The pDNA/b25k-PEI polyplexes dispersion and different PEI solutions with individual PEI chains were mixed with desired N/P ratios in the serum-free DMEM medium. The resultant solution mixtures were added to the cells at a final concentration of 0.4 μg pDNA per well. The medium was replaced with the DMEM containing 10% FBS (500 μL/well) 6 h after the addition of the polyplexes. After 48 h, the transfected HepG2 cells were lysed in Glo Lysis Buffer (Promega, USA). The luminescence of the luciferase in cell lysate and luciferin and the protein concentration of cell lysate were detected by GloMax 96 microplate luminometer (Promega, USA) and Pierce BCA protein assay kit (Thermo Scientific, USA) for each well, respectively. The gene transfection efficiency was expressed as a relative luminescence unit (RLU) per cellular protein (mean ± SD of quadruplicates). Alternatively, in vitro transgene expression was also qualitatively observed by fluorescence microscopy with pDNA pEGFP-N1 as the exogenous reporter gene.

2.4. Inhibition of endocytosis pathways

To block a certain endocytosis pathway, the HepG2 cells were pretreated with one of the following endocytosis inhibitors, Chlp (30 μM for 30 min), Wort (100 nM for 30 min), or HMA (50 μM for 5 min) in 100 μL of serum-free DMEM medium. After the pretreatment, the polyplexes with or without free PEI chains were added. After incubating for 6 h, the FBS-free medium with inhibitors and the polyplexes in each well was replaced with 500 μL DMEM containing 10% FBS. After 48 h, the RLU and protein concentration were measured by the luciferase assay and BCA assay, respectively, to calculate the gene transfection efficiency.

2.5. Confocal laser scanning microscopy (CLSM)

Each μ-Dish$^{35\ mm,high}$ (ibidi, Germany) was seeded with 100,000 cells and incubated for 24 h. In order to monitor the intracellular trafficking of the polyplexes inside HepG2 cells, pDNAs and cells were labeled as follows (Fig. 1A and D): both pGL3 and pEGFP-N1 were covalently labeled with Cy3 ($\lambda_{ex} = 550$ nm, $\lambda_{em} = 570$ nm) using the Label IT tracker Cy3 kit (Mirus, USA), lysosomes were labeled with Lamp-1 GFP ($\lambda_{ex} = 488$ nm, $\lambda_{em} = 520$ nm) via the virus-mediated transduction using CellLight lysosomes-GFP BacMam 2.0 (Molecular Probes, USA), and the nuclei were labeled with Hoechst ($\lambda_{ex} = 350$ nm, $\lambda_{em} = 461$ nm, Thermo Scientific, USA). Each labeling was performed by following the manufacturer's instruction. Then, 1.6 mL solution mixture of Cy3-polyplexes and free PEI chains in the serum-free DMEM medium was added to the cells with a final concentration of 3.2 μg pDNA/mL for each dish. Live cell images were captured using a Nikon C1si CLSM equipped with a standard fluorescence detector (Nikon, Japan) and an INU stage-top incubator (Tokai Hit, Japan). Cy3-pDNAs, GFP-lysosomes and Hoechst nuclei were excited with 543 nm, 488 nm and 405 nm lasers, respectively; and corresponding emissions were detected with 605/75 nm, 515/30 nm and 450/35 nm detectors, respectively. All the CLSM images were analyzed using the Nikon EZ-C1 software and ImageJ.
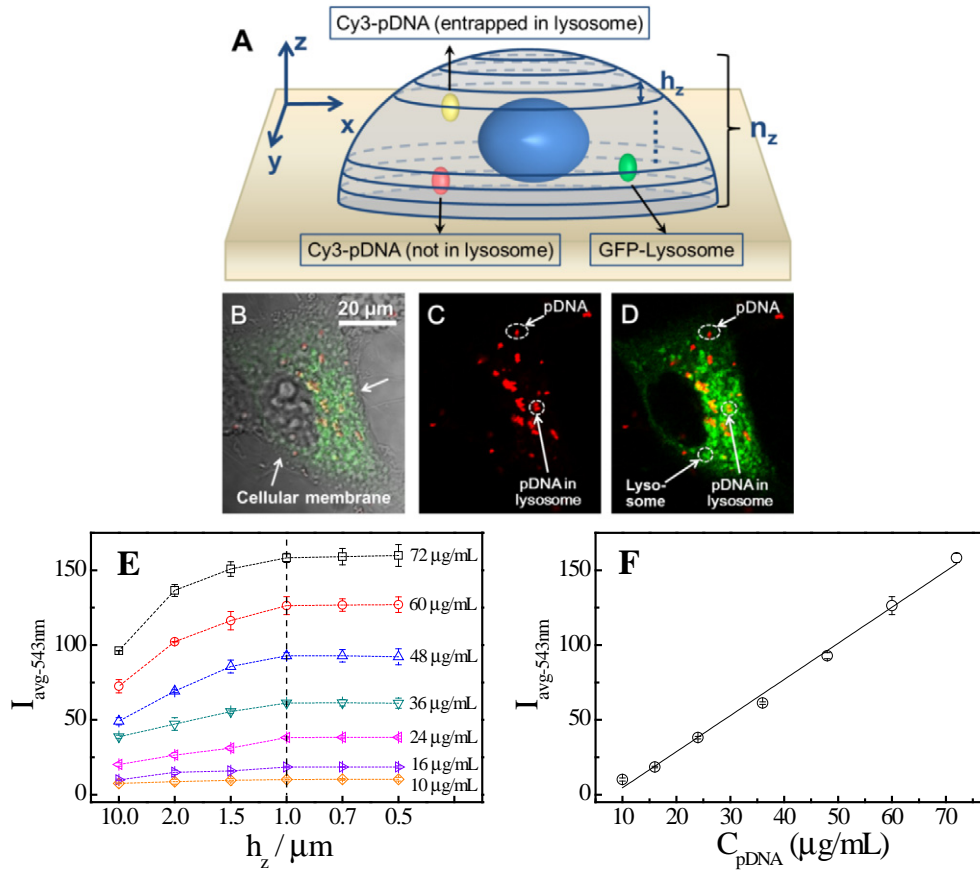
Fig. 1. (A) Schematic of a confocal image-assisted three-dimensionally integrated method to quantify cellular uptake and lysosomal distribution of polyplexes, where pDNA and lysosomes are covalently labeled with Cy3 (red) and Lamp-1 GFP (green) via virus-mediated transduction, respectively. (B–D) images of one slice (xy-plane) of a typical cell transfected with polyplexes without free cationic PEI chains after 6 h, where (B) phase-contrast image; (C) laser (543 nm) induced fluorescence image detected by 605/75 nm channel; (D) laser (488 nm and 543 nm) induced fluorescence images detected by a combination of 605/75 nm and 515/30 nm channels. (E) Effect of z-direction-step size (h_z) on average laser (543 nm) induced fluorescence intensity of a fixed volume of artificial cytoplasm, where it was scanned from bottom up with an area of 1.0×10^5 μm^2 in xy-plane. (F) pDNA concentration dependence of $I_{avg-543 \ nm}$ in 1.6 mL artificial cytoplasm [28], where the scanning volume for each sample was fixed as 318×318 μm (i.e. 1024×1024 pixel) in xy-plane and 10 μm in z-direction.

2.6. Quantification of polyplexes entrapped in lysosomes

The confocal image-assisted three-dimensionally integrated quantification (CIDIQ) method (Fig. 1A) were used to quantify the polyplexes in lysosomes [25–27]. Labeling pDNA with Cy3 (red) and lysosomes of HepG2 with GFP (green) enables us to visualize the intracellular localization of the polyplexes. The yellow clusters (an overlay of the red and green images) mark those polyplexes inside lysosomes, as shown in Fig. 1A and D. In CIDIQ, each living cell is scanned by confocal in the xy-plane from bottom to top at a fixed z-direction-step size (h_z) and the z-direction is equally divided into n_z slices. Integrating the polyplexes in lysosomes of each cell slice, we can calculate the total polyplexes in lysosomes of each cell.

To find an optimal h_z, we first prepared a series of dispersions with different polyplexes concentrations in an artificial cytoplasm in cell culture dishes and then scanned their xy-planes with different h_z values under the excitation of 543 nm laser. Fig. 1E shows that the average fluorescence intensity of the scanning cube, $I_{avg-543 \ nm}$, ($I_{avg-543 \ nm} = \sum_{i=1}^{n_z} I_{i-543 \ nm}/n_z$, where $I_{i-543 \ nm}$ is the fluorescence intensity of each z-slice) is nearly independent of h_z when $h_z \leq 1$ μm, indicating that we can use $h_z = 1$ μm in this concentration range to estimate $I_{avg-543 \ nm}$ within each cell. In this way, we established a linear relationship between $I_{avg-543 \ nm}$ and the concentration of pDNA complexed in the polyplexes (C_{pDNA}), as shown in Fig. 1F; namely,

$$I_{avg-543 \ nm} = 2.44 C_{pDNA} - 19.8 \tag{1}$$

Therefore, the amount of Cy3-pDNA complexed in the polyplexes located inside the lysosomes of each cell slice (m_{lyso}) can be calculated as

$$m_{lyso} = \sum_{i-1}^{n_z} \left(F_{lyso-i} \times C_{pDNA-i} \times S_i \times h_z \right) \tag{2}$$

where S_i is the cross-section area of the cell determined by the cellular membrane appeared in the phase-contrast image in xy-plane (Fig. 1B), and F_{lyso-i} is the fraction of polyplexes inside lysosomes of each cell slice.

To calculate the F_{lyso-i}, we used a series of 488 nm and 543 nm laser-induced fluorescence images to track those polyplexes inside lysosomes; namely, those yellow dots detected by combining 605/75 nm and 515/30 nm channels (Fig. 4D). Due to the overlapping emission spectra of GFP and Cy3 in 605/75 nm channel, the average fluorescence intensity of GFP-lysosomes within each cell ($I_{GFP-488 \ + \ 543 \ nm}$) obtained without the Cy3-polyplexes was subtracted as background. Therefore, F_{lyso-i} is calculated as

$$F_{lyso-i} = \frac{I_{lyso-488+543 \ nm} - I_{GFP-488 \ nm}}{I_{uptake-488+543 \ nm} - I_{GFP-488+543 \ nm}} \tag{3}$$

A combination of Eqs. (2) and (3) leads to the pDNA copy number inside the lysosomes (n_{lyso}).

2.7. Quantification of intracellular or intranuclear pDNA using TaqMan real-time PCR

The nuclei of the HepG2 cells transfected with pGL3 for 48 h were isolated with Nuclei EZ prep kit (Sigma-Aldrich, Germany) following the manufacturer's instruction. After washing twice with the lysis buffer as instructed by the manufacturer, the intact isolated nuclei were further washed twice with PBS containing 0.001% SDS and then twice with PBS to eliminate the contamination of nuclear membrane-associated pDNA, The nuclei were separated by 500g centrifugation at 4 °C for 5 min for each wash. The genomic DNAs (gDNAs) of the whole cells or nuclear samples were respectively extracted with the blood & cell culture DNA purification kit (Qiagen, Germany). Briefly, the samples were lysed with proteinase K for 10 min at 56 °C. After the addition of ethanol, the lysate was loaded onto the DNeasy mini spin column, where the DNA was selectively bound to the column membrane, and the contaminants were washed off with buffers. The purified DNA was eluted in water by centrifugation and used as a gDNA sample containing internalized plasmid for the TaqMan PCR assays. The probe designed to target the luciferase sequence in pGL3 is 5′-FAM-CCGCTGAATTGGAATCCATCTTGCTC-TAMRA-3′ with forward primer 5′-TTGACCGCCTGAAGTCTCTGA-3′ and reverse primer 5′-ACACC TGCGTCGAAG- ATGTTG-3′ [29]. To quantify the corresponding cell number of the tested sample, we simultaneously ran the TaqMan Copy Number reference assay (human, RNase P, Applied Biosystems, USA) as a calibrator, which targets a genomic sequence known to exist in two copies in a diploid genome. Therefore, the copy number of the intercellular or intranuclear pGL3 per cell can be determined by $2 \times 2^{\Delta C_T}$, where ΔC_T is the difference of threshold cycle values measured by PCR between the target luciferase and the reference genomic sequence.

2.8. Quantification of intracellular mRNA encoding luciferase (luc-mRNA)

The total RNA of the transfected HepG2 cells was extracted with RNeasy mini kit (Qiagen, Germany) as the manufacturer's instructions. To eliminate the gDNA contaminations, an on-column DNase digestion was performed using the RNase-free DNase set (Qiagen, Germany). The purified RNA containing luciferase mRNA was eluted in RNase-free water by centrifugation. The concentrations of the isolated gDNA and RNA were calculated from their absorbance at 260 nm. The RNAs were converted into their complementary DNAs (cDNA) via the reverse transcription with PrimeScript RT master mix (Takara, Japan). The resultant cDNA encoding luciferase was detected by real-time PCR with the same set of TaqMan primers and probe mentioned before, which target the luciferase sequence in pGL3. The luciferase control RNA (1 mg/mL, Promega, USA) was used as an external reference. The absolute copy number of the luc-mRNA in the total RNA sample can be derived from the relationship between the number of cycles (C_T) associated with cDNA transcribed from the luciferase control RNA and the copy number of the luciferase control RNA calculated using the transcript size of 1.8 kbp [47]. In addition, we detected the β-actin mRNA as an internal reference with Human Beta Actin Endogenous Control (Applied Biosystems, UK) by real-time PCR. Since the β-actin can be stably expressed no matter whether free cationic PEI chains are added or not, the amount of cellular β-actin mRNA linearly correlated to the initial cell number of the RNA sample tested in each reaction. The absolute copy number of luc-mRNA per cell was calculated as the ratio of number of luc-mRNA to the initial cell numbers in each reaction.

2.9. Quantification of intranuclear luc-mRNA

The nuclear luc-mRNA in each reaction was estimated with an external reference, luciferase control RNA as described before. Since adding free PEI chains may affect the distribution of β-actin mRNA within the cell, we cannot directly use the internal reference, nuclear β-actin

mRNA to estimate the cell number in each reaction. Dividing the amount of nuclear β-actin mRNA by the amount of cellular β-actin mRNA for a fixed initial number of cells, we obtained the fraction of nuclear β-actin mRNA under each experimental condition: 8.7% and 1.7%, transfected with N/P = 3 and 10, respectively. Using these data, we were able to convert the amount of nuclear β-actin mRNA into the amount of cellular β-actin mRNA and thus calculated the cell number of each reaction. Consequently, the absolute copy number of nuclear luc-mRNA per cell was quantified by the ratio of nuclear luc-mRNA copy number to the cell number in each reaction.

3. Results and discussion

Fig. 2 shows the effects of length and topology of free cationic PEI chains on the transgene expression of pGL3 complexed with b25k-PEI. A comparison of the transfection efficiency of pGL3/b25k-PEI polyplexes (N/P = 3) without free PEIs and those with different kinds of free cationic PEI chains (N/P = 10, 7 portions are free in the solution mixture) shows that after 48 h, the transfection efficiency generally reaches its corresponding maximum [12,13], but the addition of free cationic PEI chains increases the transfection efficiency by a factor of ~500 times. Here the chain length plays a vital role; namely, long free cationic PEI chains are much more effective than short ones. For free chains with a lower molar mass, linear ones are more effective than branched ones. However, when the chains reach a certain length (~15–20 nm), the chain topology makes little difference. The promoting efficacy of free chains follows the order of b25k-PEI ~ lin25k-PEI > lin2.5 k-PEI > b2k-PEI.

We have hypothesized that those long free cationic chains penetrated and adsorbed on the cellular and organelle membranes interfere with the signal proteins (v-SNARE and t-SNARE) so that the cell could not recognize the ingested polyplexes as foreign subjects so that they could detour the effective endosome-lysosome pathway and avoid the lysosomal entrapment [13,30]. In this way, the polyplexes would have a much lower chance to be digested and a higher chance to be translocated into nucleus. On the other hand, the penetration and adsorption of long cationic chains on different membranes cause the leak of cytosol, leading to cytotoxicity [31–34]. Our previous study reveals that at N/P = 7 (C_{PEI} = 1.8 μg/mL), >75% cells are survived even after 48 h with 10% or less LDH releasing in spite of different chain lengths and topologies [25], leading us to conclude that this amount of free cationic PEI chains used for gene transfection has no significant destabilizing effect on the membrane integrity.
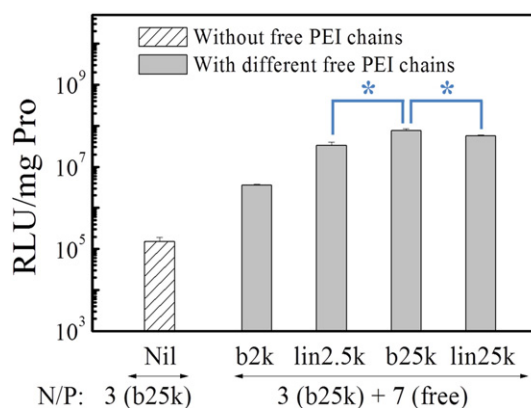

Fig. 2. Effects of length and topology of free cationic PEI chains on gene transfection in HepG2 cells without or with 7 portion (N/P = 7) of different free cationic PEI chains, where pDNA is complexed with 3 portion (N/P = 3) of b25k-PEI. b2k, b25k, lin2.5k and lin25k indicate branched PEI with an M_w of 2000 and 25,000 g/mol, and linear PEI with an M_w of 2500 and 25,000 g/mol, respectively. Significant results are indicated by * if $0.01 < p < 0.05$ (n = 4, Student's t-test).

We have previously studied two different polyplexes endocytic pathways in Hela cells, i.e., the clathrin- and the caveolae-mediated endocytosis, and found that without free long cationic chains to disrupt the caveolae-mediated pathway, the gene transfection efficiency was significantly low, but disrupting the clathrin-mediated pathway has little effect on the gene transfection [25,35]. Since HepG2 is deficient in caveolin [36,37], we refocus our attention on the macropinocytosis. Using different inhibitors to selectively block specific endocytic pathways, we are able to determine which pathway was mainly employed to internalize the polyplexes by HepG2 cells. Among them, chlorpromazine hydrochloride (Chlp) inhibits the clathrin-mediated pathway by interacting with the plasma membrane protein to reduce the clathrin-coated pits [38]; 5-(N,N-hexamethylene) amiloride (HMA) and wortmannin (Wort) block the macropinocytosis by respectively inhibiting the sodium-proton exchange [39] and the phosphatidylinositol 3-kinase [40].

Fig. 3A shows that without free cationic chains (N/P = 3), blocking the clathrin-mediated endocytosis with Chlp has nearly no effect on the transfection efficiency; but blocking macropinocytosis results in a remarkably lower transfection efficiency after 48 h, revealing that the polyplexes mainly enter HepG2 cells via the macropinocytosis pathway because there is no specific ligand on the polyplexes surface. Fig. 3A also shows that the transfection efficiency even slightly increases by 5% when the clathrin-mediated pathway is blocked by Chlp ($p < 0.01$, significantly different from "Nil"), suggesting that more polyplexes enter the cells via macropinocytosis, a more favorable pathway for the ligand-free polyplexes. Our results are consistent with the early reported advantages of macropinocytosis, including the increase of the cell uptake and the avoidance of the lysosomal degradation [41–43].

On the other hand, with free cationic PEI chains (N/P = 10), the transfection efficiency only decreases by ~50% even though macropinocytosis is inhibited by either HMA or Wort. In principle, after blocking macropinocytosis, the polyplexes most likely enter the cells via the clathrin-mediated pathway in which the polyplexes should be delivered to lysosomes via the endosome-lysosome pathway so that the transfection efficiency would be very low. The fact that the transfection efficiency only decreases ~50% shows that free cationic chains reduce the lysosome entrapment. The assumption is supported by the fact that after blocking the clathrin-mediated pathway by Chlp, we see nearly no effects on the transfection efficiency ($p > 0.05$) even with free cationic chains because the polyplexes do not enter the cells via the clathrin-mediated pathway in this case so that free cationic chains provide no help in avoiding the lysosome entrapment. Our results clearly reveal that the promotion of the gene transfection mainly occurs inside the cell; namely, the avoidance of the lysosome entrapment. In other words, the current results are consistent with our hypothesis that long free cationic chains on the anionic membranes can interfere with the signal SNARE proteins to disrupt the intravesicular fusion between lysosomes and the polyplexes-containing vesicles ingested via the clathrin-mediated or macropinosomes pathway so that the hydrolysis inside lysosomes can be reduced or avoided [43–45]. It is understandable that the gene transfection efficiency dramatically decreases when both the pathways are blocked, as shown in Fig. 3B.

To further investigate how the chain-length and topology of cationic polymers affect the final transfection efficiency during intracellular trafficking, we first quantified the cellular uptake at 6 h after the addition of the polyplexes by TaqMan real-time PCR. The cellular uptake in 6 h is considered as the final amount of internalized polyplexes because the cellular uptake of the polyplexes detected by the flow cytometry with or without different free PEI chains reaches its maximum in 6 h, [12] and we replaced the polyplexes-containing FBS-free DMEM medium with complete culture medium at 6 h. Fig. 4 shows that without free PEI chains the HepG2 cells can internalize 1.15×10^5 copies pGL3 per cell and that the addition of free PEI chains has no significant effect on the cellular uptake ($p > 0.05$, n = 3, Student's t-test, compared with N/P = 3), indicating that free cationic chains mainly promote the transfection inside the cell.

The next barrier on the intracellular trafficking pathway of the polyplexes is the lysosomal entrapment. Using the confocal image-assisted three-dimensionally integrated quantification method (CIDIQ) [25–27], we quantified the polyplexes entrapped inside the lysosomes. Without free cationic chains, the pGL3 entrapped inside lysosomes (n_{lyso}) reaches its maximum 7.6×10^4 copies per cell in 6 h (shown as dotted lines in Fig. 5A to D), i.e., ~66% of the total intracellular pGL3 (Fig. 5E). The addition of short free b2k-PEI chains has nearly no effect on the copy number of pGL3 inside lysosomes (Fig. 5A and E, $p > 0.05$), showing that short branched free cationic chains are not able to effectively block the endosome-lysosome pathway. In contrast, adding free lin2.5k-, b25k- or lin25k-PEI chains greatly reduces F_{lyso} to ~30% and n_{lyso} reaches a steady value after 2–3 h (Fig. 5B–E, $p < 0.01$), clearly revealing that long free cationic chains reduce the lysosomal entrapment, i.e., more than half of those polyplexes destined toward lysosomes are detoured so that their lysosomal entrapment/degradation are avoided. It is worth noting that although b2k-PEI and lin2.5k-PEI share similar molar mass, lin2.5k-PEI (~18 nm if stretched) is much longer than b2k-PEI (~6 nm) [13,30,46]. Since the ingestion and digestion of pDNA inside the lysosomes take place simultaneously and have reached the equilibrium point after 6 h under each experimental condition, we use the n_{lyso} in 6 h to estimate the effects of free cationic chains on the avoidance of lysosomal entrapment.

A comparison of the number of the polyplexes inside the cells shows that longer free PEI chains (lin2.5k-, b25k- and lin25k-PEI) are more effective in preventing the lysosomal entrapment, up to 2.4 times when long free b25k-PEI chains are used. Note that long free b25k-PEI chains promote the overall gene transfection efficiency by a factor of ~500 times. Therefore, free cationic chains must play more important roles in helping pDNA to overcome other intracellular barriers.

Fig. 6 shows that up to 30 min, short b2k-PEI chains are still on the cellular membrane, whereas long free b25k-PEI chains has already translocated into the cells and localized in some intracellular vesicles. After 1 h, long b25k-PEI has much higher fluorescence intensity than short b2k-PEI. These results are consistent with our previous studies
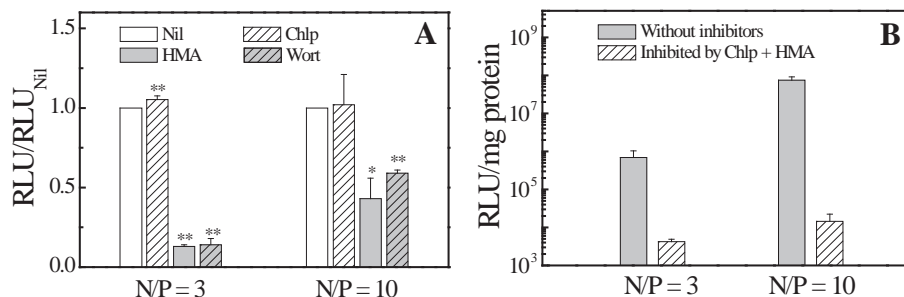

Fig. 3. Effects of (A) clathrin-mediated endocytic inhibitor (Chlp) and Macropinocytic inhibitors (HMA and Wort) and (B) blocking both macropinocytosis and clathrin-mediated endocytosis on transgene pGL3 expression in HepG2 cells without (N/P = 3) and with 7-portion of free b25k-PEI chains (N/P = 10) after 48 h, where "Nil" means no inhibitors without (N/P = 3) and with (N/P = 10) free b25k-PEI chains, respectively. Significant results are indicated by * if $0.01 < p < 0.05$, and ** if $p < 0.01$ (n = 4, Student's t-test).
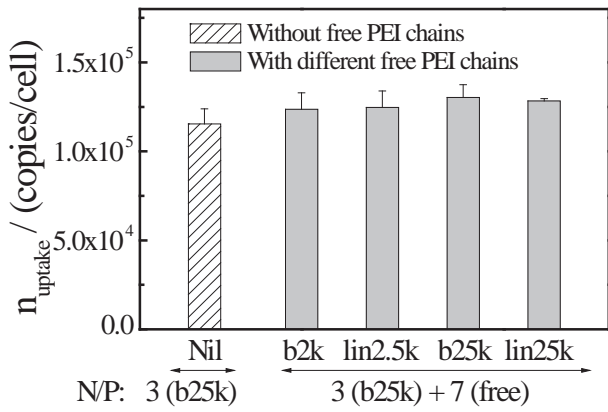
Fig. 4. Effects of different free cationic PEI chains on HepG2 cellular uptake of polyplexes in 6 h, where n_{uptake} is copy number of intracellular pGL3, and "Nil" results without free PEI chains.

[25,31]. We have hypothesized that free cationic chains can prevent the lysosomal entrapment by penetrating/absorbing on the membrane of different organelles and interacting with SNARE membrane proteins that signal the inter-vesicular fusion of different organelles so that the inter-vesicular endosome-lysosome fusion is disrupted. Our previous studies revealed that cationic chains with a size larger than 15 nm can effectively disrupt the inter-vesicular fusion. Note that the size of b2k-PEI is ~6 nm [13,25]. However, cationic chains longer than 20 nm become more toxic to the cells because they disrupt all the membranes, especially that of mitochondrion.

Hereafter, we will only discuss the effect of long free b25k-PEI chains because they are more effective than other types of PEI chains in promoting the transgene expression. For those ingested polyplexes that successfully avoid the lysosomal entrapment, the next major hurdle is the transportation of those pDNAs into nuclei. We quantified those intranuclear pDNA chains in 48 h by the TaqMan real-time PCR. As shown in Fig. 7A, the addition of long free b25k-PEI chains increases intranuclear pGL3 from 4.2×10^3 to 5.0×10^4 copies per cell, suggesting
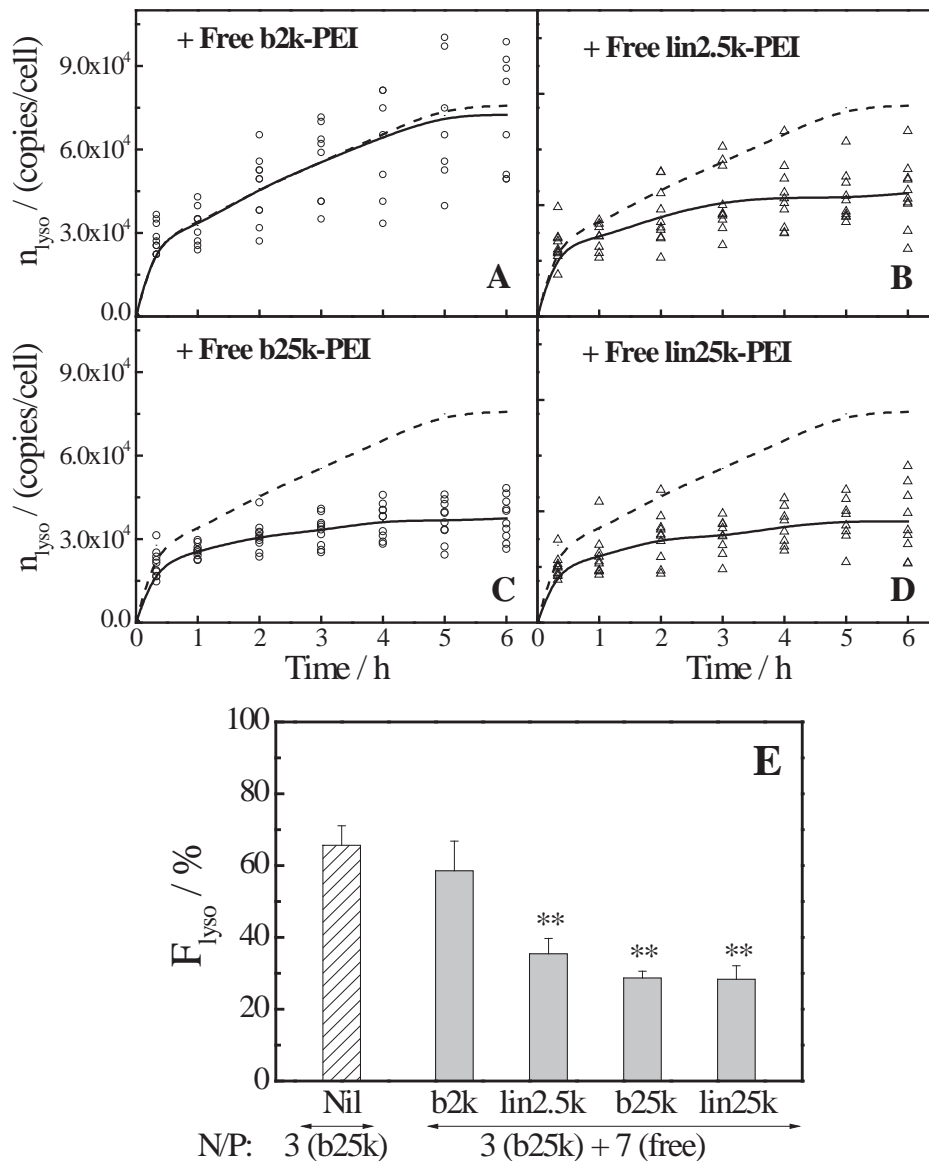

Fig. 5. (A)–(D) Time dependence of lysosomal entrapment of polyplexes without and with different free cationic chains, where 10 cells were analyzed under each experimental condition; small hollow symbols: n_{lyso} of a single cell at different times; and dotted (no free chains) and continuous (with free chains) lines: 10-cell averaged values of n_{lyso}. (E) Comparison of effects of different free cationic PEI chains on lysosomal entrapment of those polyplexes inside each cell (F_{lyso}) in 6 h, where significant results are indicated by * if $0.01 < p < 0.05$, and ** if $p < 0.01$ (n = 10, Student's t-test).
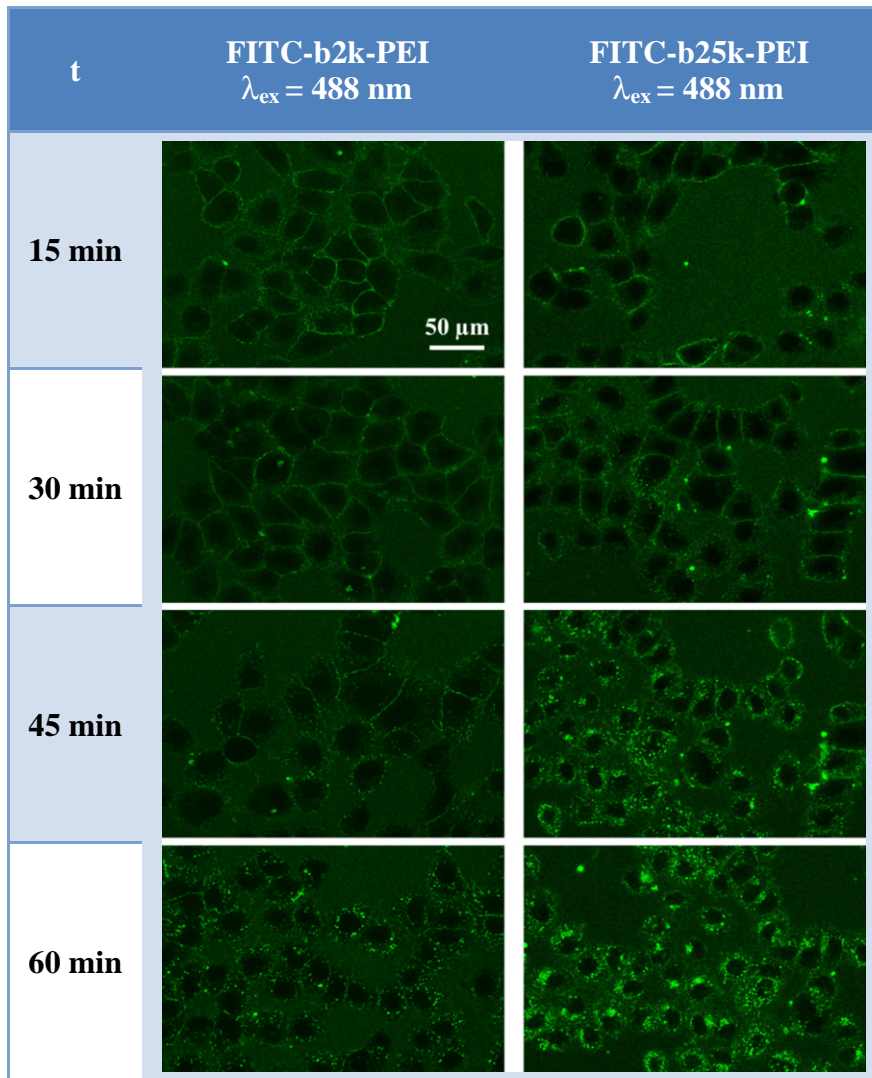
Fig. 6. Internalization and intracellular trafficking of FITC-labeled b2k-PEI and b25k-PEI chains in the HepG2 cells, where the concentration of FITC-PEI is 1.8 μg/mL in serum-free DMEM; t is time after addition of FITC-PEI; and FITC is excited with 488-nm laser and detected with 450/35 nm channel.

that the cumulative effect of free b25k-PEI chains after the nuclear entry is ~12 folds that consists of 2.4 folds on the avoidance of the lysosome entrapment and 5.0 folds on the translocation of pDNA through nuclear membrane.

Note that we also measured the fluorescence intensity of Cy3-pDNA by the confocal microscope in 48 h and found that the intranuclear pGL3 calculated by CIDIQ method are 2.2×10^2 copies and 6.6×10^2 copies per cell without and with free cationic chains, respectively, as shown
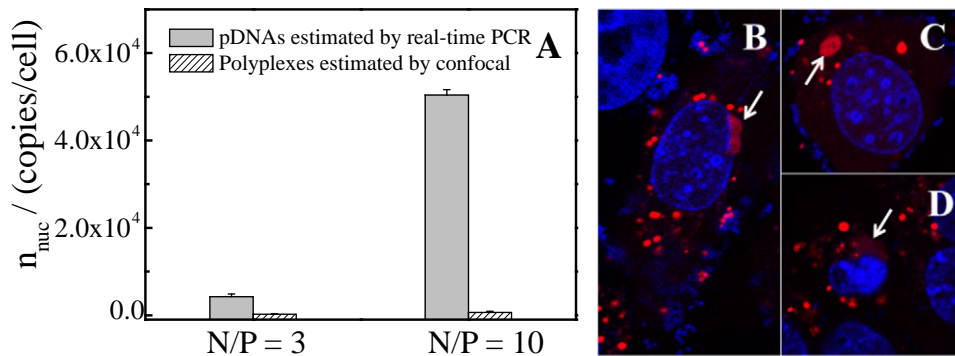
Fig. 7. (A) Effects of free cationic b25k-PEI chains on nuclear transportation of pDNAs in 48 h after adding polyplexes; and (B)–(D) confocal images of typical HepG2 cells transfected by polyplexes (red) with free b25k-PEI chains after 24 h, where nuclei were labeled with Hoechst (blue); large dim red areas indicated by arrows nearby each nucleus show polyplexes with a loose structure or partially released Cy3-pEGFP-N1; and images were captured simultaneously with 605/75 nm and 515/30 nm channels.

in Fig. 7A, much lower than those measured by the TaqMan real-time PCR because the confocal method mainly sees the condensed Cy3-pDNA inside the polyplexes not those released from the polyplexes while the TaqMan PCR method detects individual free pDNA chains. Putting these results together, we conclude that pDNAs must exist as individual chains inside each nucleus rather than the complexed chains inside the polyplexes. In other words, most of the pDNA chains inside the polyplexes are released before their translocation through the nuclear membrane.

Another evidence to support the above conclusion is some large dim red areas observed around the nuclei labeled with Hoechst (blue) inside those cells successfully transfected (cytosol with expressed green EGFP) by the Cy3-pEGFP-N1/b25k-PEI polyplexes (red), as shown in Fig. 7B–D. Those large dim red areas indicate that the polyplexes become loose and the labeled pDNA chains are released around the nuclei. Our results confirm that pDNAs inside the nuclei exist as individual pDNA chains, free from the complexations, and large free cationic PEI chains promote the final translocation of pDNA through the nuclear membrane after pDNA is released from the polyplexes nearby nucleus.

Further, the mRNA encoding luciferase (luc-mRNA) is quantified by the TaqMan PCR assay. As shown in Table 1, the addition of free b25k-PEI chains dramatically increases the final cellular luc-mRNA in 48 h by ~49 times (2.0×10^4 and 9.8×10^5 copies/cell without and with free b25k-PEI cationic chains, respectively). To estimate the sole effect of free PEI chains on the transcription stage, we compared the transcription efficiencies, i.e., the ratio of the cellular luc-mRNA copy number to the nuclear pGL3 copy number, with and without free PEI chains and found that the transcription efficiencies are 20 and 4.8 times, respectively.
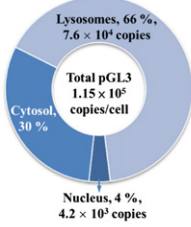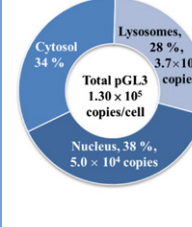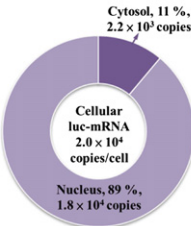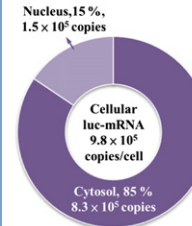
Considering that luc-mRNA has to be exported from the nucleus into the cytosol prior to translation, we quantified the cellular luc-mRNA distribution by TaqMan PCR with β-actin as an internal reference to evaluate the effect of free b25k-PEI chains on the translocation of luc-mRNA. The results reveal that the final cytosolic luc-mRNA in 48 h in the presence of free b25k-PEI chains (8.3×10^5 copies/cell) is ~380 folds of that with no free b25k-PEI chains (2.2×10^3 copies/cell), comparable to the overall transfection efficiency (~500 folds) with and without free cationic chains (shown in Table 2). If we eliminate the contributions in those preceding stages (the lysosome entrapment, the cytosol-to-nucleus transportation of pDNA and the transcription), the sole effect of free cationic chains on the translocation of luc-mRNA is about 7.7 times. It is worth-noting that the addition of free cationic chains has nearly no effect on the ratio of the nuclear luc-mRNA to its internal reference, nuclear β-actin mRNA. In other words, free cationic chains has a similar effect on the translocation of β-actin mRNA, indicating that the promotive effect of free cationic chains on the translocation of mRNA from nucleus to cytosol is nonspecific. The promotive effect of free b25k-PEI on the nuclear entry of pDNA and export of mRNA is presumably attributed to its disruption of the nuclear membrane [48,49].

Table 1
Quantitative comparison of transcription efficiency of pDNA and translocation of luciferase mRNA without and with free b25k-PEI chains.

	Without free PEIs NP = 3	With free b25k-PEIs NP = 10
Transcription of pDNA		
Nuclear pGL3 (copies/cell)	4.2×10^3	5.0×10^4
Cellular luc-mRNA (copies/cell)	2.0×10^4	9.8×10^5
Transcription efficiency	4.8	20
Translocation of luc-mRNA		
Nuclear luc-mRNA (copies/cell)	1.8×10^4	1.5×10^5
Cytosolic luc-mRNA (copies/cell)	2.2×10^3	8.3×10^5

Table 2
Summary of effects of free b25k-PEI chains on intracellular trafficking of polyplexes, cytosol-to-nucleus transportation of pDNAs, transcription of pDNAs into mRNAs, and translocation of mRNAs during transgene expression, where each cell initially has, on average, 3.2×10^6 pGL3 copies.

	Without free PEIs (N/P = 3)	With free PEIs (N/P = 10)	Effect of free PEIs
Transfection efficiency	1.5×10^5 RLU/mg pro	7.5×10^7 RLU/mg pro	**500 ± 60 folds**
Stage 1 pGL3 intracellular trafficking + **Stage 2** pGL3 cytosol-to-nucleus transportation	Lysosomes, 66%, 7.6×10^4 copies; Total pGL3 1.15×10^5 copies/cell; Cytosol, 30%; Nucleus, 4%, 4.2×10^3 copies	Lysosomes, 28%, 3.7×10^4 copies; Cytosol 34%; Total pGL3 1.30×10^5 copies/cell; Nucleus, 38%, 5.0×10^4 copies	2.4 folds × 5.0 folds
Stage 3 Transcription efficiency	4.8	20	4.1 folds
Stage 4 mRNA nucleus-to-cytosol translocation	Cytosol, 11%, 2.2×10^3 copies; Cellular luc-mRNA 2.0×10^4 copies/cell; Nucleus, 89%, 1.8×10^4 copies	Nucleus, 15%, 1.5×10^5 copies; Cellular luc-mRNA 9.8×10^5 copies/cell; Cytosol, 85% 8.3×10^5 copies	7.7 folds
The overall effect of Stages 1–4: 380 ± 80 folds			

4. Conclusions

In this study, we found that free cationic chains can remarkably promote the transgene expression by helping the pDNAs inside the polyplexes to overcome each of the intracellular barriers in different stages, including the intracellular trafficking of the polyplexes, the cytosol-to-nucleus transportation of pDNAs, the transcription from pDNAs to mRNAs and the nucleus-to-cytosol translocation of mRNAs. Namely, additional free cationic chains (b2k-, lin2.5k-, b25k- and lin25k-PEIs) have little effects on the cellular uptake of the polyplexes but disrupt the lysosomal entrapment and degradation of the polyplexes, in which free cationic chains with a size larger than 15 nm, such as branched PEI chains with a molar mass of 25,000 g/mol, is more effective so that the overall number of the polyplexes in the cytosol increases 2.4 times. Further, free cationic chains enhance the cytosol-to-nucleus transportation of pGL3 5.0 times in those transfected HepG2 cells and increase the transcription efficiency 4.1 times. More importantly, free cationic chains help the translocation of luc-mRNA from nuclei into cytosol by a factor of 7.7 folds. The cumulative effect of free cationic b25k-PEI chains on the enhancement of the gene transfection is 380 times in comparison with that without free cationic chains. This cumulative enhancement calculated on different stages is comparable with the experimentally observed total transgene expression (~500 times), indicating that the promoting effects of free cationic chains on the gene transfection mainly occur before the translation. The promotion effect of free cationic chains on each stage of the gene transfection follows the following order: the intracellular trafficking of the polyplexes < the transcription of pDNAs < the cytosol-to-nucleus transportation of pDNAs < the nucleus-to-cytosol translocation of mRNAs.

Acknowledgments

References

[1] R. Mulligan, The basic science of gene therapy, Science 260 (1993) 926–932.
[2] C.E. Thomas, A. Ehrhardt, M.A. Kay, Progress and problems with the use of viral vectors for gene therapy, Nat. Rev. Genet. 4 (2003) 346–358.
[3] H. Yin, R.L. Kanasty, A.A. Eltoukhy, A.J. Vegas, J.R. Dorkin, D.G. Anderson, Non-viral vectors for gene-based therapy, Nat. Rev. Genet. 15 (2014) 541–555.
[4] F. Mingozzi, K.A. High, Therapeutic in vivo gene transfer for genetic disease using AAV: progress and challenges, Nat. Rev. Genet. 12 (2011) 341–355.
[5] M.A. Mintzer, E.E. Simanek, Nonviral vectors for gene delivery, Chem. Rev. 109 (2008) 259–302.
[6] S.C. De Smedt, J. Demeester, W.E. Hennink, Cationic polymer based gene delivery systems, Pharm. Res. 17 (2000) 113–126.
[7] Y. Zhang, A. Satterlee, L. Huang, In vivo gene delivery by nonviral vectors: overcoming hurdles & quest, Mol. Ther. 20 (2012) 1298–1304.
[8] D.W. Pack, A.S. Hoffman, S. Pun, P.S. Stayton, Design and development of polymers for gene delivery, Nat. Rev. Drug Discov. 4 (2005) 581–593.
[9] V.A. Bloomfield, DNA condensation by multivalent cations, Biopolymers 44 (1997) 269–282.
[10] J.N. Kizhakkedathu, A.L. Creagh, R.A. Shenoi, N.A.A. Rossi, D.E. Brooks, T. Chan, J. Lam, S.R. Dandepally, C.A. Haynes, High molecular weight polyglycerol-based multivalent mannose conjugates, Biomacromolecules 11 (2010) 2567–2575.
[11] S. Boeckle, K. von Gersdorff, S. van der Piepen, C. Culmsee, E. Wagner, M. Ogris, Purification of polyethylenimine polyplexes highlights the role of free polycations in gene transfer, J Gene Med 6 (2004) 1102–1111.
[12] Y. Yue, F. Jin, R. Deng, J. Cai, Y. Chen, M.C. Lin, H.F. Kung, C. Wu, Revisit complexation between DNA and polyethylenimine - effect of uncomplexed chains free in the solution mixture on gene transfection, J. Control. Release 155 (2011) 67–76.
[13] Y. Yue, F. Jin, R. Deng, J. Cai, Z. Dai, M.C. Lin, H.F. Kung, M.A. Mattebjerg, T.L. Andresen, C. Wu, Revisit complexation between DNA and polyethylenimine–effect of length of free polycationic chains on gene transfection, J. Control. Release 152 (2011) 143–151.
[14] O. Boussif, F. Lezoualc'h, M.A. Zanta, M.D. Mergny, D. Scherman, B. Demeneix, J.-P. Behr, A versatile vector for gene and oligonucleotide transfer into cells in culture and in vivo: polyethylenimine, Proc. Natl. Acad. Sci. 92 (1995) 7297–7301.
[15] R. Kircheis, L. Wightman, E. Wagner, Design and gene delivery activity of modified polyethylenimines, Adv. Drug Deliv. Rev. 53 (2001) 341–358.
[16] U. Lungwitz, M. Breunig, T. Blunk, A. Gopferich, Polyethylenimine-based non-viral gene delivery systems, Eur. J. Pharm. Biopharm. 60 (2005) 247–266.
[17] W.T. Godbey, K.K. Wu, A.G. Mikos, Size matters: molecular weight affects the efficiency of poly(ethylenimine) as a gene delivery vehicle, J. Biomed. Mater. Res. 45 (1999) 268–275.
[18] M. Ogris, P. Steinlein, M. Kursa, K. Mechtler, R. Kircheis, E. Wagner, The size of DNA/transferrin-PEI complexes is an important factor for gene expression in cultured cells, Gene Ther. 5 (1998) 1425–1433.
[19] L. Wightman, R. Kircheis, V. Rossler, S. Carotta, R. Ruzicka, M. Kursa, E. Wagner, Different behavior of branched and linear polyethylenimine for gene delivery in vitro and in vivo, J Gene Med 3 (2001) 362–372.
[20] F.R. Maxfield, T.E. McGraw, Endocytic recycling, Nat. Rev. Mol. Cell Biol. 5 (2004) 121–132.
[21] J. Gruenberg, H. Stenmark, The biogenesis of multivesicular endosomes, Nat. Rev. Mol. Cell Biol. 5 (2004) 317–323.
[22] T. Bieber, W. Meissner, S. Kostin, A. Niemann, H.-P. Elsasser, Intracellular route and transcriptional competence of polyethylenimine–DNA complexes, J. Control. Release 82 (2002) 441–454.
[23] B. Yu, X. Zhao, L.J. Lee, R.J. Lee, Targeted delivery systems for oligonucleotide therapeutics, AAPS J. 11 (2009) 195–203.
[24] S. Brunner, E. Fürtbauer, T. Sauer, M. Kursa, E. Wagner, Overcoming the nuclear barrier: cell cycle independent nonviral gene transfer with linear polyethylenimine or electroporation, Mol. Ther. 5 (2002) 80–86.
[25] Y. Yanan, Quantitative comparison of endocytosis and intracellular trafficking of DNA/polymer complexes in the absence/presence of free polycationic chains, How

[26] H. Akita, R. Ito, I. Khalil, S. Futaki, H. Harashima, Quantitative three-dimensional analysis of the intracellular trafficking of plasmid DNA transfected by a nonviral gene delivery system using confocal laser scanning microscopy, Mol. Ther. 9 (2004) 443–451.
[27] S. Hama, H. Akita, R. Ito, H. Mizuguchi, T. Hayakawa, H. Harashima, Quantitative comparison of intracellular trafficking and nuclear transcription between adenoviral and lipoplex systems, Mol. Ther. 13 (2006) 786–794.
[28] R.V. Benjaminsen, H. Sun, J.R. Henriksen, N.M. Christensen, K. Almdal, T.L. Andresen, Evaluating nanoparticle sensor design for intracellular pH measurements, ACS Nano 5 (2011) 5864–5873.
[29] S. Hama, H. Akita, S. Iida, H. Mizuguchi, H. Harashima, Quantitative and mechanism-based investigation of post-nuclear delivery events between adenovirus and lipoplex, Nucleic Acids Res. 35 (2007) 1533–1543.
[30] Y. Yue, C. Wu, Progress and perspectives in developing polymeric vectors for in vitro gene delivery, Biomaterials Science 1 (2013) 152–170.
[31] J. Cai, Y. Yue, D. Rui, Y. Zhang, S. Liu, C. Wu, Effect of chain length on cytotoxicity and endocytosis of cationic polymers, Macromolecules 44 (2011) 2050–2057.
[32] A. Hémar, A. Subtil, M. Lieb, E. Morelon, R. Hellio, A. Dautry-Varsat, Endocytosis of interleukin 2 receptors in human T lymphocytes: distinct intracellular localization and fate of the receptor alpha, beta, and gamma chains, J. Cell Biol. 129 (1995) 55–64.
[33] M. Breunig, U. Lungwitz, R. Liebl, A. Goepferich, Breaking up the correlation between efficacy and toxicity for nonviral gene delivery, Proc. Natl. Acad. Sci. U. S. A. 104 (2007) 14454–14459.
[34] H. Lv, S. Zhang, B. Wang, S. Cui, J. Yan, Toxicity of cationic lipids and cationic polymers in gene delivery, J. Control. Release 114 (2006) 100–109.
[35] J. Rejman, A. Bragonzi, M. Conese, Role of clathrin- and caveolae-mediated endocytosis in gene transfer mediated by lipo- and polyplexes, Mol. Ther. 12 (2005) 468–474.
[36] L.C. Matthews, M.J. Taggart, M. Westwood, Effect of cholesterol depletion on mitogenesis and survival: the role of caveolar and noncaveolar domains in insulin-like growth factor-mediated cellular function, Endocrinology 146 (2005) 5463–5473.
[37] R. Qi, D.G. Mullen, J.R. Baker, M.M. Holl, The mechanism of polyplex internalization into cells: testing the GM1/caveolin-1 lipid raft mediated endocytosis pathway, Mol. Pharm. 7 (2010) 267–279.
[38] L.-H. Wang, K.G. Rothberg, R. Anderson, Mis-assembly of clathrin lattices on endosomes reveals a regulatory switch for coated pit formation, J. Cell Biol. 123 (1993) 1107–1117.
[39] M.S. Weinberg, S. Nicolson, A.P. Bhatt, M. McLendon, C. Li, R.J. Samulski, Recombinant adeno-associated virus utilizes cell-specific infectious entry mechanisms, J. Virol. 88 (2014) 12472–12484.
[40] M.P. Wymann, G. Bulgarelli-Leva, M.J. Zvelebil, L. Pirola, B. Vanhaesebroeck, M.D. Waterfield, G. Panayotou, Wortmannin inactivates phosphoinositide 3-kinase by covalent modification of Lys-802, a residue involved in the phosphate transfer reaction, Mol. Cell. Biol. 16 (1996) 1722–1733.
[41] J.S. Wadia, R.V. Stan, S.F. Dowdy, Transducible TAT-HA fusogenic peptide enhances escape of TAT-fusion proteins after lipid raft macropinocytosis, Nat. Med. 10 (2004) 310–315.
[42] I.A. Khalil, K. Kogure, S. Futaki, H. Harashima, High density of octaarginine stimulates macropinocytosis leading to efficient intracellular trafficking for gene expression, J. Biol. Chem. 281 (2006) 3544–3551.
[43] I.A. Khalil, K. Kogure, H. Akita, H. Harashima, Uptake pathways and subsequent intracellular trafficking in nonviral gene delivery, Pharmacol. Rev. 58 (2006) 32–45.
[44] S. Mayor, R.E. Pagano, Pathways of clathrin-independent endocytosis, Nat. Rev. Mol. Cell Biol. 8 (2007) 603–612.
[45] R.A. Petros, J.M. DeSimone, Strategies in the design of nanoparticles for therapeutic applications, Nat. Rev. Drug Discov. 9 (2010) 615–627.
[46] Z. Dai, C. Wu, How does DNA complex with polyethylenimine with different chain lengths and topologies in their aqueous solution mixtures? Macromolecules 45 (2012) 4346–4353.
[47] D.R. Johnson, P.K. Lee, V.F. Holmes, L. Alvarez-Cohen, An internal reference technique for accurately quantifying specific mRNAs by real-time PCR with application to the tceA reductive dehalogenase gene, Appl. Environ. Microbiol. 71 (2005) 3866–3871.
[48] G. Kabachinski, T.U. Schwartz, The nuclear pore complex–structure and function at a glance, J. Cell Sci. 128 (2015) 423–429.
[49] A. Lam, D. Dean, Progress and prospects: nuclear import of nonviral vectors, Gene Ther. 17 (2010) 439–447.

Free Cationic Polymer Chains Promote Gene Transfection, Springer International Publishing, Heidelberg 2013, pp. 73–94.